

# Analysis of digital timing methods with DRS4 board\*

DU Cheng-Ming(杜成名)<sup>1,2</sup> CHEN Jin-Da(陈金达)<sup>1,1)</sup> YANG Hai-Bo(杨海波)<sup>1,2</sup>

CHENG Ke(成科)<sup>1,3</sup> ZHANG Xiu-Ling(张秀玲)<sup>1</sup> XU Hu-Shan(徐珊珊)<sup>1</sup>

HU Zheng-Guo(胡正国)<sup>1</sup> SUN Zhi-Yu(孙志宇)<sup>1</sup>

<sup>1</sup>Institute of Modern Physics, Chinese Academy of Sciences, Lanzhou 730000, China

<sup>2</sup>University of Chinese Academy of Sciences, Beijing 100049, China

<sup>3</sup>Northwest Normal University, Lanzhou 730070, China

## Abstract:

Digital Pulse Processing (DPP) modules are being used to replace the analog electronics modular in modern physics experiments for processing the original signals from detectors. A new DPP modules based on domino ring sampler version 4 (DRS4) and multiple methods for processing arrival times are presented in this paper. In the experiments, the detectors were irradiated with 511keV  $\gamma$  ray from a  $^{22}\text{Na}$  source. The detectors consists of  $\text{LaBr}_3$  scintillators ( $\Phi 20 \times 5 \text{mm}^3$ ) and XP20D0 Photomultiplier Tubes(PMTs), and the acquiring system was a 8+1 channels DRS4 board. Multiple DPP including (1)leading-edge discrimination, (2)constant-fraction zero-crossing discrimination and (3)digital constant fraction discrimination were investigated. The best time resolution is 194.7ps FWHM, obtained by constant fraction discrimination method, which is better than the other DPP methods and the traditional analog systems using the same detectors. The DRS4 board and DPP methods can be applied to supplement positron emission tomography (PET) with time of flight (TOF) for better localization of the positron annihilation, and they can also be used for the scintillation timing measurement with picosecond accuracy, such as TOF- $\Delta E$  and TOF-E detectors for particle identification.

**Key words:**digital pulse processing,DRS4,waveform sampling,time resolution,TOF, $\text{LaBr}_3$

**PACS:**29.40.mc, 78.70.Bj,84.37.+q

## 1 Introduction

Digital Pulse Processing (DPP) modules are being used more often to analyze detector signals. Advantages include: reducing drift, archiving of data for later analysis, and better controlling over analysis parameters. The maximum informations of the pulse from detector can be acquired by digitizing a fast signal directly, for example, the drift time and pulse area can be easily obtained from the waveform. The DRS4 chip[1], which has been designed at the Paul Scherrer Institute, Switzerland, is a cheap, switched capacitor array(SCA)[2] that is capable of sampling eight differential input channels at a sampling speed of 0.7 to 5 gigabit samples per second (GSPS).

---

\*This work was supported by the Science Foundation of the Chinese Academy of Sciences (210340XBO), National Natural Science Foundation of China (11305233,11205222), General Program of National Natural Science Foundation of China (11475234) and Specific Fund of National Key Scientific Instrument and Equipment Development Project (2011YQ12009604).

1)E-mail:chenjinda@impcas.ac.cn

In order to simplify the design process to integrate the DRS4 chip into TOF-PET system, a eight channels boards based on DRS4 chip has been designed and developed by Nuclear Electronics Group in Institute of Modern Physics, Chinese Academy of Sciences. It is basically equivalent to a eight channel 5GSPS digital oscilloscope and its input range can be adjusted to match different kinds of detector signals. And the internal time resolution between channels is about 50ps[3].

In this paper the DRS4 board was tested in coincidence timing measurements using fast scintillators and PMTs. In the experiments, the difference of the arrival time of two coincident  $^{22}\text{Na}$   $\gamma$  rays were detected by two  $\text{LaBr}_3$  detectors coupled with XP20D0s[4,12], by the means of the various DPP techniques and the analog method.

The DPP techniques includes (1) leading-edge discrimination(LED)[5], (2) constant fraction zero-crossing discrimination(CFD)[6,8,9] and (3) digital constant fraction discrimination(dCFD)[6,8]. Each technique was repeated multiple times to optimize the parameters for the best resolution and accuracy. The analog method were using the constant-fraction zero-crossing technique for the comparison with DPP techniques

## 2 Experiment setup

Two  $\phi 20\text{mm} \times 5\text{mm}$   $\text{LaBr}_3$  scintillators coupled with XP20D0s were placed apart with  $^{22}\text{Na}$  source for 511keV  $\gamma$  ray test. The voltages between the anode and cathode were increased to get a linearity photoelectric signals output with the applied supply voltages of 1400V. The source was in an aluminum holder with a 2 mm lead collimating aperture placed on an aluminum track. The holder was placed at L, M, R points step by step and data were collected by DRS4 and CAMAC systems as shown in Fig 1. The expected difference of the arrival time ( $\delta t$ ) for the signal is  $\delta t = 2d/c$ , In the formula,  $c$  means the speed of light,  $d$  is the moving distance for the the  $^{22}\text{Na}$  source. By moving the source with a distance of 20cm, it is expected that the mean time values of the two peaks of the arrival times distributions from the L point and R point should be 1.333ns[6].

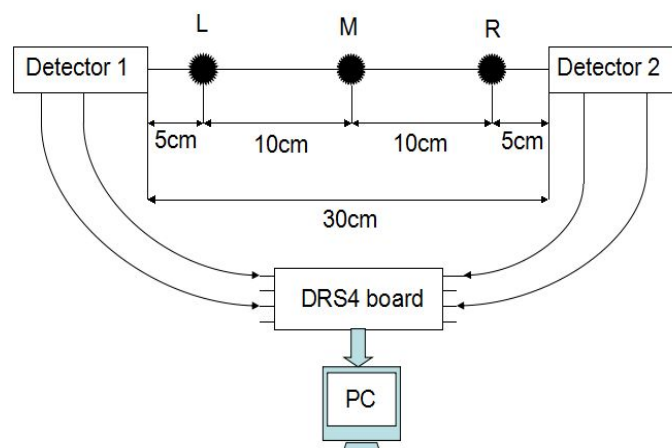


Fig. 1. Schematic diagram of the DRS4 system and two  $\text{LaBr}_3$  detectors.  
(L M R means the holder are placed at the left side, middle point and right side )

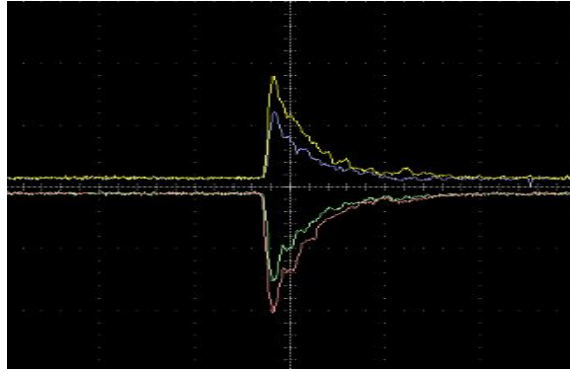


Fig. 2 Four output waveforms shown on the screen of the DRS4 interface .  
(The positive pulses represent the Dynode signals and the negative pulses represent the Anode signals from the two  $\text{LaBr}_3$  detectors)

The dynode pulses of the PMTs are directly sent to ch0 and ch1 and the anode pulses are sent to ch2 and ch3 of the DRS4 board. In the internal triggering mode, if the voltages of chn0 signal and chn1 signal exceed the default thresholds in the default time period, the trigger state will on . The continuous pulses of the input signals are digitally converted to discrete waveform data and stored in the memories of the DRS4 board after the trigger state is on. The shapes of the dynode and anode signals from the two  $\text{LaBr}_3$  detectors acquiring by DRS4 system are shown in Fig 2.

The waveform data were acquired by the DRS4 board working at the sampling rate of 5.12 Gs/s with an individual channel depth of 1024 and the sampling time interval was 200ps. The full time scale range of each input channel is about 200ns in this paper.

An analog accruing system with traditional NIM electronic modules and CAMAC system was also used as a comparison with DRS4 system to determine the difference of pulse arrival times.

### 3 Digital analysis methods and Results

#### 3.1 Waveform Reconstruction

The waveform information is stored in the following forms , such as the Amplitude[1024] and Time[1024]. The original 2-byte integers voltage values and 4-byte floating point effective time bin widths are converted to ROOT data following the decoding rules[7], then the data can be used to construct the waveform. Fig.3 illustrates the reconstructed energy signal(anode-negative pulse) and time signal(cathode-positive pulse) for the  $\text{LaBr}_3$  detectors.

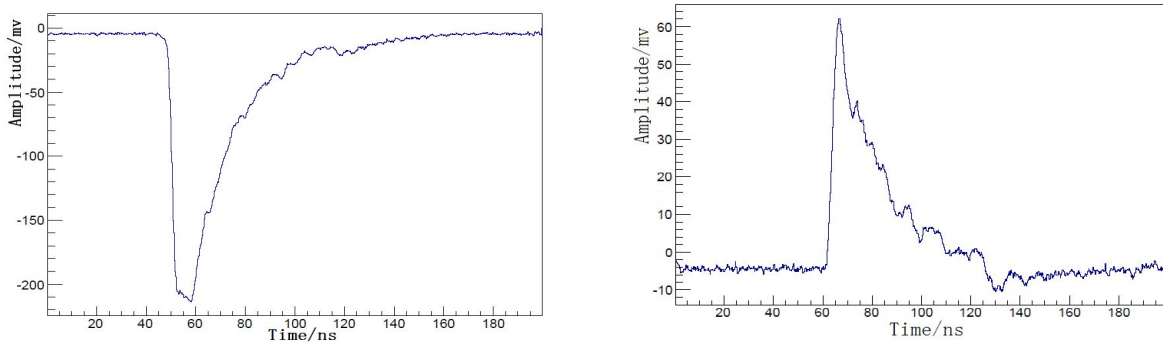


Fig.3 The reconstructed energy signal(anode-negative pulse) and time signal(cathode-positive pulse) from the  $\text{LaBr}_3$  detector by DRS4 original data.

### 3.2 Energy spectrum and amplitude spectrum

In the traditional experimental methods, the total energy of the measured pulse is proportional to the sum of all created scintillation photons, the pulse area between the digitized waveform and the baseline is relevant to  $\gamma$  ray energy. The value of the pulse area is calculated by digital integration method, which is simply to sum the amplitude value of each channel over the whole waveform range in our experiment.

The photon-peak of the spectrum is normalized to 511 keV. In the analog system, the energy spectrum distributions of integrating the pulse area are illustrated in Fig. 4. The photon-peak is clearly separated from the Compton scattering, and the energy resolutions at 511 keV are measured to be 4.25% (FWHM) and 4.60% (FWHM), respectively for the two detectors.

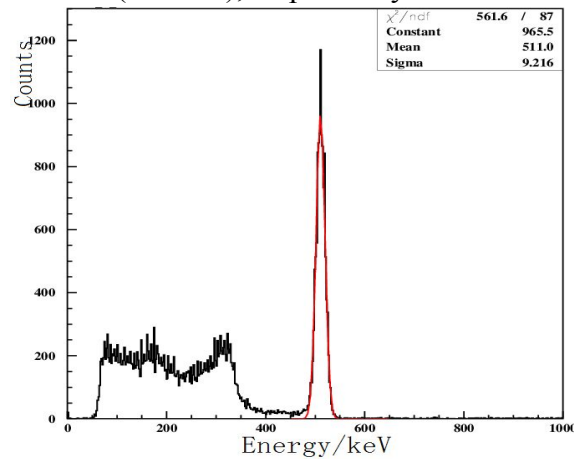


Fig.4 The  $\gamma$  ray energy distributions obtained by analog system with  $^{22}\text{Na}$  source and the energy resolutions is 4.25% (FWHM).

In the DRS4 the energy spectrum distributions of integrating the pulse area are performed in Fig. 5. The obtained energy resolutions at 511 keV is 3.42% (FWHM) and 4.10% (FWHM). It can be seen that the difference between the analog and digital is small, but the resolution for the DRS4 system is better than analog system.

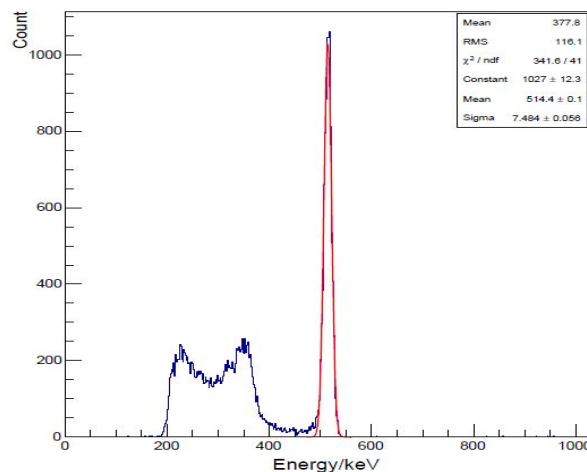


Fig.5 The  $\gamma$  ray energy distributions obtained by DRS4 system with  $^{22}\text{Na}$  source and the energy resolutions is 3.42% (FWHM).

The energy and amplitude discriminator windows are dependent on the energy and amplitude

distribution as showed in Fig 5 and Fig.6. Only those pulses whose energy and amplitude stayed in the range of the energy and amplitude windows would subsequently be analyzed. The signal below 400 keV are attributed to Compton scattered photons. Events in the 511 keV peak ranger were used for the analysis of the TOF information. The energy window [490,530] keV for energy signals and amplitude window [75,95] mv for time signals were chosen to extract the suitable signals for timing analysis.

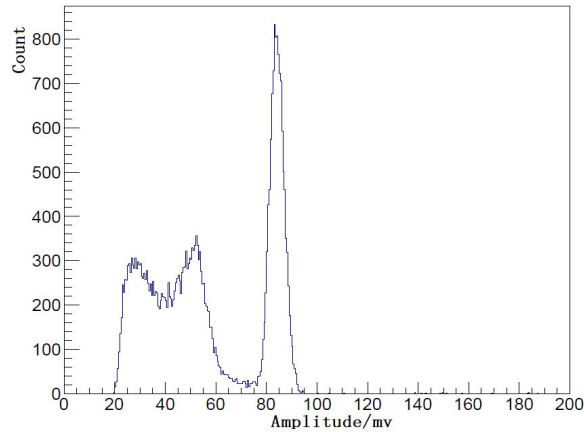


Fig.6 The amplitudes of time signals from LaBr3 detector obtained by DRS4 system with  $^{22}\text{Na}$  source for  $\gamma$  rays test distributions

### 3.3 The internal distributions of arrival times difference and time resolution

The precision of the timing measurement is performed by the delay time measurement based on the cable delay method. The distribution of delay intervals tested is illustrated in Fig.7. The internal time resolution between channels is about 52ps[3,7].

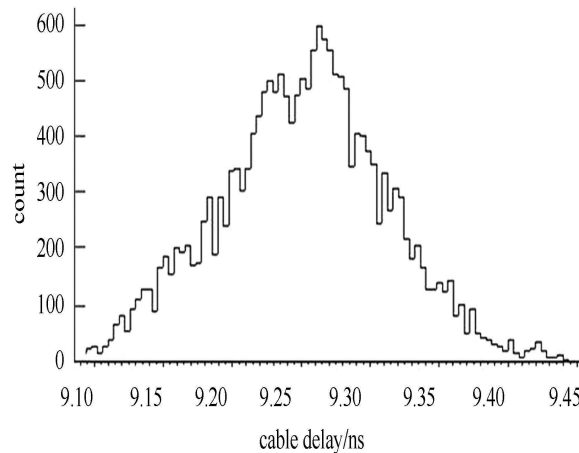


Fig .7 The difference distribution of arrive times obtained based on cable delay method

### 3.4 Analysis of digital timing methods

The calculated difference of the arrival time ( $\delta t$ ) for the two detector pulses is 1.334ns in DRS4 system when the  $^{22}\text{Na}$  source was placed respectively at L, R points as showed in Fig 1 . The result is very conform with the expected arrival time :1.333ns. The difference of the arrival time ( $\delta t$ ) obtained by analog method is 1.331ns, and the best time resolution is 254.7ps.

It is generally believed that the best timing algorithm for scintillation detector pulses is the

constant fraction discrimination timing method. This method analyses the result of numerous leading-edge-timing measurements according to the moment that represents the minimum time jitter when the pulse crosses a certain constant fraction level of its full amplitude. The optimum fraction is a characteristic of the detectors, the scintillator, and the PMT types. Various DPP methods are performed to compare with the constant fraction discrimination method to obtain the distribution of arrive times difference and time resolution.

### 3.4.1 Leading-edge discrimination(LED) method

The simplest digital method is the leading-edge discrimination. The first 200 samples of each waveform were averaged and subtracted from the rest of the waveform to compensate for any DC offset. Two adjacent sample points  $(a_1, t_1)$ ,  $(a_2, t_2)$  nearby threshold level whose amplitudes satisfied the inequality of  $a_1 < \text{threshold} < a_2$  were chosen for each signals[6,9]. Then a linear interpolation[4] was operated between  $(a_1, t_1)$  and  $(a_2, t_2)$  to estimate the actual zero-crossing time  $T_1(T_2)$  for each time pulse as showed in Fig.8. In this paper the thresholds were set equal to 6% of the mean values of pulses amplitudes in 511keV peaks area to obtain the distributions of arrive times difference  $(T_1 - T_2)$  between two time pulses from two  $\text{LaBr}_3$  detectors. The distribution of arrival times difference and the best time resolution is: 210.9ps(FWHM) by Gaussia fit as showed in Fig.9.

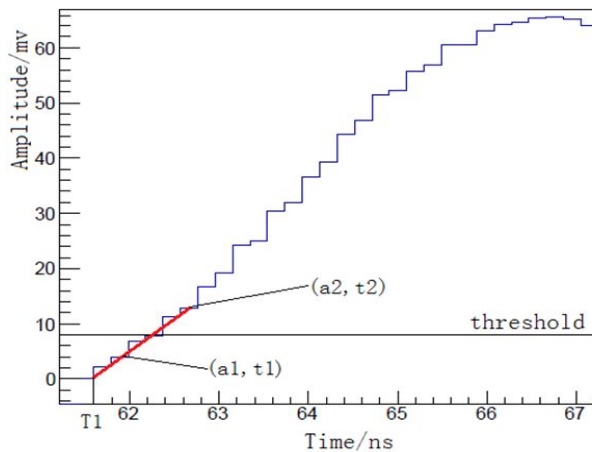


Fig.8 The sketch of the linear interpolation to estimate the actual zero-crossing time  $T_1$  for LED and DCFD methods.

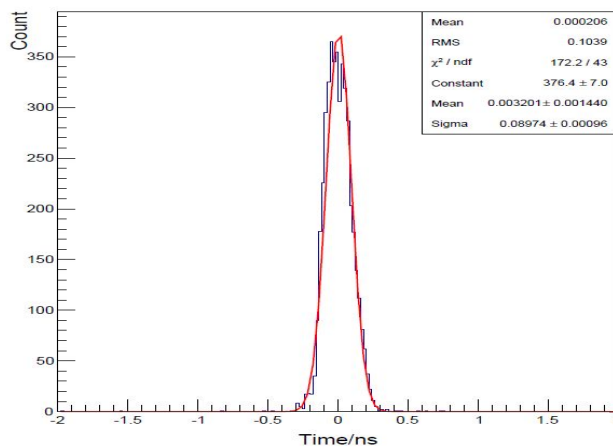


Fig.9 The distribution of arrival times difference obtained by LED method and the best time resolution: 210.9ps(FWHM) by Gaussia fit.

### 3.4.2 Constant-fraction discrimination(CFD) method

The constant-fraction-zero-crossing method is used by many analog systems to measure the arrival time of the detector signals. It is a very complicated process and needs a lot of hardware. However, the digital technique makes it easy to implement the constant-fraction discrimination method without modifying the original signal. The CFD method searches for the maximum digitized value (MDV) of the pulse and then sets a threshold ( $V_{th}$ ) based on a predefined fraction ( $p$ ) of the MDV in this paper [6,8,9]. With the same way of the LED method, the rest of the program estimates the actual zero-crossing time  $T_1$  ( $T_2$ ) for each time signal as illustrated in Fig. 8. In the experiments, the threshold was set equal to 6% of the MDV to obtain the distributions of arrival times difference ( $T_1 - T_2$ ) between two time pulses from two  $\text{LaBr}_3$  detectors. The distribution of arrival times difference and the best time resolution is: 194.7 ps (FWHM) by Gaussian fit as shown in Fig. 11.

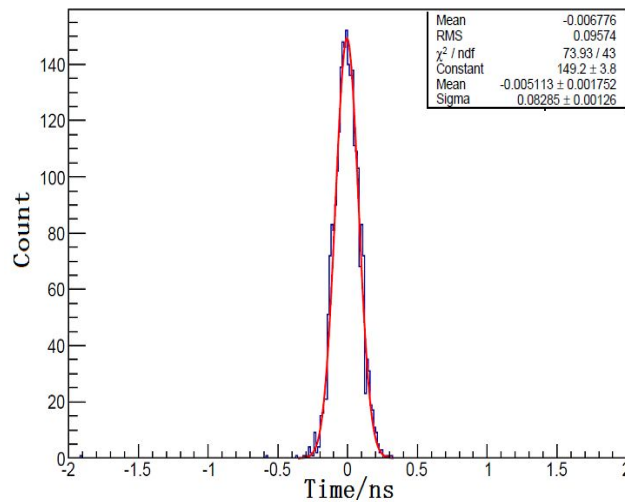


Fig. 10 The distribution of arrival times difference obtained by CFD method and the best time resolution: 194.7 ps (FWHM) by Gaussian fit.

### 3.4.3 Digital Constant-fraction zero-crossing (dCFD) method

This method is the digital version for the analog CFD method. In the process, the original signal is delayed from 1 to 5 time steps, amplified and inverted at first. Then the processed signal is added to the original signal. After this process, the unipolar signal is optimized and transformed into a bipolar pulse. The bipolar pulse crosses the time-axis at a constant fraction of the height of the original pulse [6,9]. The zero-crossing time ( $T_1$ ) is linearly interpolated between  $(a_1, t_1)$  and  $(a_2, t_2)$  whose amplitudes satisfy the inequality of  $a_1 > 0 > a_2$  as shown in Fig. 11. The distribution of arrival times difference and the best time resolution is: 229.3 ps (FWHM) by Gaussian fit as shown in Fig. 12.

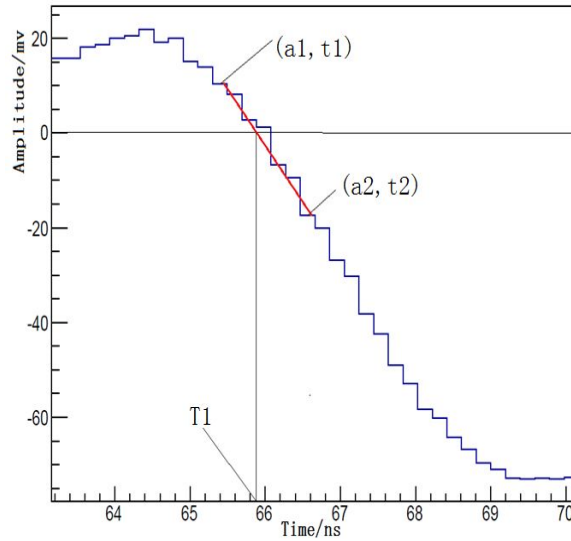


Fig.11 The sketch of the linear interpolation(red line)between (a1, t1) and (a2, t2) to estimate the actual zero-crossing time T1 for dCFD method.

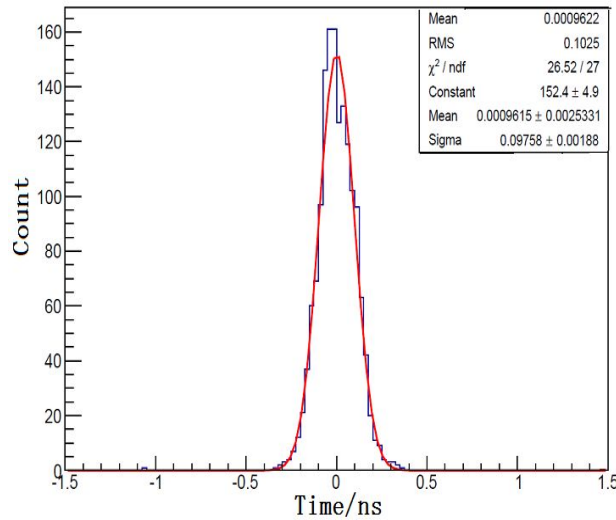


Fig.12 The distribution of arrival times difference obtained by dCFD method and the best time resolution:229.3ps(FWHM) by Gaussia fit.

Considering the precision and the computer processing speed(according to the operation times of algorithms), CFD method was finally adopted.

We studied the dependent parameters[6,8] of the time resolution both on the fit range and the constant-fraction factor  $p$  which is equal to  $V_{th}/MDV$  in the experiment. The numbers of points used in the analysis before and after the  $V_{th}$  are varied in order to optimize the resolution and the accuracy. These are referred to as pre- $V_{th}$  and post- $V_{th}$ , respectively.

The relationship between  $p$  and the time resolution is illustrated in Table.1. While the relationship between fitting range and the time resolution is shown in Table.2. The Table.1 shows constant-fraction factor between 3% to 10% do not make much difference for time resolution. The best time resolution obtained is 194.7ps(FWHM) with setting the threshold :6% of MDV when the fitting ranger was pre- $V_{th}=4$  and post- $V_{th}=3$ .

Table 1. The relationship between Constant-fraction factor(P) and the time resolution.

P	Time resolution/ps	Error/ps
2%	212.8	3.08
3%	199.9	2.89
5%	198.5	2.87
6%	194.7	2.96
7%	198.0	3.08
10%	200.6	2.90
15%	202.5	2.98
25%	210.6	3.24

Table2. The relationship between fitting ranger and the time resolution.

Fitting ranger	Time resolution/ps	Error/ps
Pre- $V_{th}=5$ Post- $V_{th}=5$	200.69	3.06
Pre- $V_{th}=4$ Post- $V_{th}=4$	195.12	2.73
Pre- $V_{th}=4$ Post- $V_{th}=3$	194.7	2.72
Pre- $V_{th}=4$ Post- $V_{th}=2$	197.14	2.84
Pre- $V_{th}=4$ Post- $V_{th}=1$	199.38	2.89
Pre- $V_{th}=2$ Post- $V_{th}=3$	201.49	3.08
Pre- $V_{th}=3$ Post- $V_{th}=3$	197.47	2.87
Pre- $V_{th}=3$ Post- $V_{th}=2$	198.36	2.89

#### 4 Discussions and Conclusions

A pair of LaBr<sub>3</sub> scintillator detectors and a DRS4 board have been set up and tested in this paper. The ability of different timing methods to process the arrival time of a digitized radiation detector signals has been examined, and the best time resolution for the system is 194.7ps(FWHM), which obtained with the CFD method with the constant-fraction factor :6% and the fitting ranger: Pre- $V_{th}=4$  Post- $V_{th}=3$  .

The experiment results show that the time performance of the digital system based on the DRS4 board with CFD method is the best method among LED ,dCFD and analog system (254.7ps FWHM) mehtods in this work,also litter better than those published results,such as 195.4ps FWHM by mean PMT pulse model[9] and 206ps FWHM by Gaussian rising edge fitting method[4,6,9].And according to algorithms of each digital methods,the CFD method is the fastest calculating speed.

Some drawbacks for DRS4 such as :limited sampling depth(not enough for microsecond level signal) and large amount of data have been found in this experiment. Some proposals have been offered to solve those problems:multi-channels cascaded to extend sampling depth and sending the extracted time and energy information, instead of the whole waveform. We also can anticipate the DRS5[10] board for solving those problems.

The DRS4 system is less expensive, and it does not require additional electronics for pulse height analysis. An algorithm, which allows to define the signal's leading edge and to get a time

measurement point as close as possible to the base line, provides the best time resolution. The excellent performance demonstrates that this system has good time resolution (less than 200ps) to supplement PET with TOF for better localization of the positron annihilation to improve the quality of medical images and reduce exposure times. Next step we will apply DRS4 board and CFD methods to readout silicon photo-multipliers (SiPMs) for TOF-PET system [11] and for timing measurement for particle identification [12].

### Acknowledgements

This work is supported by the Foundation of the Chinese Academy of Sciences (210340XBO), the National Natural Science Foundation of China (11305233, 11205222), General Program of National Natural Science Foundation of China (11475234), Youth Innovation Promotion Association, CAS (201330YQO) and Specific Fund of National key scientific instrument and equipment development project (2011YQ12009604).

- [1] Ritt, S. IEEE Nuclear Science Conference Record, 2008, 1512-1515.
- [2] Ritt S, Dinapoli R, Hartmann U. Nucl. Instr. and Methods A, 2010, 623(1): 486-488.
- [3] YANG Hai-Bo, SU Hong, KONG Jie, CHENG Ke, CHEN Jin-Da, DU Cheng-Ming, ZHANG Jing-Zhe. Chinese Physics C, 2015, Vol.39(5):056101.
- [4] AN Ran, CHEN Bin, LIU Yan-Fen, YE Bang-Jiao, KONG Wei, Stefan Ritt. Chinese Physics C, 2014, Vol.38(5):056001.
- [5] Mehmet Aykac, Inki Hong, Sanghee Cho. Nucl. Instr. and Methods A, 2010, 623: 1070-1081.
- [6] Mark A. Nelson, Brian D. Rooney, Derek R. Dinwiddie, Glen S. Brunson, Nucl. Instr. and Methods A, 2003, 505:324-327.
- [7] Paul Scherrer Institute, DRS4 Evaluation Board User's Manual, 2014
- [8] L. Bardelli, G. Poggi, M. Bini, G. Pasquali, N. Taccetti. Nucl. Instr. and Methods A, 2004, 521:480 - 492.
- [9] CHEN Ze, HU Zheng-Guo, CHEN Jin-Da, et al. Nuclear Physics Review, 2015, Vol 32(2), to be published.
- [10] S. Ritt, Picosecond Workshop 2011, <http://drs.web.psi.ch/docs>.
- [11] A. Ronzhin et al. Nucl. Instr. and Methods A, 2013, 703:109 - 113.
- [12] Dustin Anderson, Artur Apreysan, et al. Nucl. Instr. and Methods A, 2015, 787:94 - 97.